CHAPTER 13

Lagrange Multiplier Approach to Fictitious Domain Methods: Application to Fluid Dynamics and Electro-Magnetics*

Q. V. Dinh[1]
R. Glowinski[2]
Jiwen He[3]
V. Kwock[1]
T. W. Pan[4]
J. Périaux[1]

We discuss in this article the numerical solution of boundary value problems from Physics and Engineering by fictitious domain/Lagrange multiplier methods. These methods are combined to finite element methods to obtain algorithms, which on the basis of preliminary numerical experiments look robust and accurate. Application to elliptic problems, to the time dependent incompressible Navier-Stokes equations and to the Helmholtz equations are discussed in details, including the results of numerical experiments used to validate the methodology investigated here.

1. Introduction

Fictitious Domain Methods for Partial Differential Equations have shown recently a most interesting potential for solving complicated problems from Science and Engineering (see, for example, [1] for some striking illustrations of the above statement). One of the main reasons of this popularity of fictitious domain methods (they are sometimes called *domain imbedding methods*; cf. [2]) is that they allow the use of fairly structured meshes on a simple shape auxiliary domain containing the actual one, allowing therefore the use of fast solvers.

[1]Dassault Aviation, Saint-Cloud, France.
[2]University of Houston, Texas and Université Paris VI, France.
[3]Dassault Aviation, Saint-Cloud and Université Paris VI, France.
[4]University of Houston, Texas.

On the other hand, the method is not without some complications; in particular, we have to compute and store the intersection of the actual boundary with the neighboring mesh elements. However these tasks are localized at the actual boundary and they may be fully automatized, whatever is the geometry (see [3] for more details and applications to transonic flow calculations).

In this paper we discuss a family of fictitious domain methods which are based on the explicit utilization of Lagrange multipliers defined on the actual boundary and associated to the genuine boundary conditions. The resulting methodology has definitely the flavor of panel methods, which have been quite popular for the simulation of inviscid incompressible potential flows.

The remainder of this article has been divided into three sections: In Section 2 we introduce the multiplier/fictitious domain methodology by considering the solution of a Dirichlet model problem.

In Section 3 we consider the Lagrange multiplier/fictitious domain solution of the Navier-Stokes equations modelling incompressible viscous flow; indeed this section generalizes — from our point of view — the methods described in [4] concerning the fictitious domain solution of the Stokes problem. Finally, in Section 4 we address the solution of the harmonic Helmholtz and Maxwell equations. The method discussed there is an alternative to the fictitious domain/control methods described in [5]. Some other numerical results are also presented.

2. A fictitious domain/Lagrange multiplier method for the linear Dirichlet problem.

2.1 Formulation. Generalities.

Motivated by the solution of the Navier-Stokes equation we consider the following Dirichlet problem

$$\alpha u - \nu \Delta u = f \text{ in } \omega, \tag{2.1}$$

$$u = g \text{ on } \gamma, \tag{2.2}$$

where α (resp. ν) is a nonnegative (resp. positive) number, and where f and g are defined over ω and γ, respectively, ω being a bounded domain of $\mathbf{R}^d$ ($d \geq 1$) and γ its boundary. Problem (2.1), (2.2) has a

unique solution and assuming that $f \in L^2(\omega)$, $g \in H^{1/2}(\gamma)$ we can show that u is also the solution of the *following variational problem*

$$(2.3) \qquad \begin{cases} u \in V_g, \\ \int_\omega (\alpha uv + \nu \nabla u \cdot \nabla v) dx = \int_\omega f v dx, \ \forall v \in H_0^1(\omega), \end{cases}$$

with

$$V_g = \{v | v \in H^1(\omega), \ v = g \ on \ \gamma\}.$$

2.2 A fictitious domain approach to the solution of problem (2.1), (2.2), (2.3).

Let us consider a "box" Ω such that $\overline{\omega} \subset \Omega$ (see Figure 2.1), and denote by Γ the boundary of Ω.

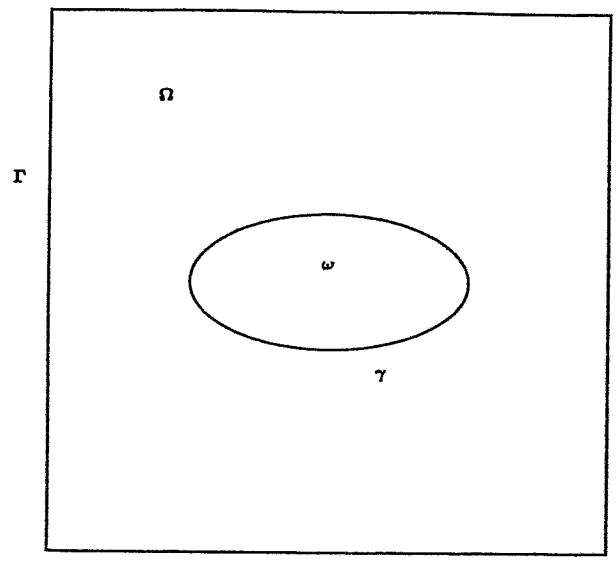

Figure 2.1

We have then equivalence between (2.1), (2.2), (2.3) and the *saddle-point* problem:

Find $\{\tilde{u}, \lambda\} \in V \times H^{-1/2}(\gamma)$ *such that*

$$\int_\Omega (\alpha \tilde{u} v + \nu \nabla \tilde{u} \cdot \nabla v) dx = \int_\Omega \tilde{f} v dx + <\lambda, v>, \quad \forall v \in V, \tag{2.4}$$

$$<\mu, \tilde{u} - g> = 0, \quad \forall \mu \in H^{-1/2}(\gamma), \tag{2.5}$$

where $\tilde{f} \in L^2(\Omega)$ and satisfies $\tilde{f}|_\omega = f$, where $<\cdot,\cdot>$ denotes the duality pairing between $H^{-1/2}(\gamma)$ and $H^{1/2}(\gamma)$ and where V is a well chosen subspace of $H^1(\Omega)$. Natural choices for V are $H^1(\Omega)$, $H^1_0(\Omega)$ and

$$H^1_p(\Omega) = \{v | v \in H^1(\Omega), \ v \textit{ periodic at } \Gamma\}.$$

We have then

$$\tilde{u}|_\omega = u. \tag{2.6}$$

Remark 2.1: The pair $\{\tilde{u}, \lambda\}$ solution of (2.4), (2.5) is a saddle-point over $V \times H^{-1/2}(\gamma)$ of the Lagrangian functional $\mathcal{L}$: $H^1(\Omega) \times H^{-1/2}(\gamma) \longrightarrow \mathbb{R}$ defined by

$$\mathcal{L}(v, \mu) = \frac{1}{2} \int_\Omega (\alpha |v|^2 + \nu |\nabla v|^2) dx - \int_\Omega \tilde{f} v dx - <\mu, v - g>. \tag{2.7}$$

2.3 Iterative solution of problem (2.4), (2.5).

For simplicity, we take $V = H^1_0(\Omega)$. The conjugate gradient algorithm to be described in this paragraph relies on the following

Proposition 2.1: *The multiplier* λ *is solution of the boundary equation*

$$A\lambda = \beta \tag{2.8}$$

where A *is a strongly elliptic isomorphism from* $H^{-1/2}(\gamma)$ *onto* $H^{1/2}$ *and where* $\beta \in H^{1/2}(\gamma)$.

Proof: Define operator A as follows

(i) To $\mu \in H^{-1/2}(\gamma)$ we associate the solution u_μ of the following elliptic variational problem

$$(2.9) \qquad \begin{cases} u_\mu \in V \\ \int_\Omega (\alpha u_\mu v + \nu \nabla u_\mu \cdot \nabla v)dx = <\mu, v>, \ \forall v \in V, \end{cases}$$

which has a unique solution.

(ii) Define A by

$$(2.10) \qquad A\mu = u_\mu|\gamma.$$

Operator A clearly belongs to $\mathcal{L}(H^{-1/2}(\gamma), H^{1/2}(\gamma))$; we also have

$$(2.11) \qquad <\mu', A\mu> = \int_\Omega (\alpha u_\mu u_{\mu'} + \nabla u_\mu \cdot \nabla u_{\mu'})dx, \ \forall \mu, \mu' \in H^{-1/2}(\gamma),$$

which implies in turn that A is *self-adjoint* and *strongly elliptic* over $H^{-1/2}(\gamma)$.

Next we define u_o by

$$(2.12) \qquad \begin{cases} u_o \in V, \\ \int_\Omega (\alpha u_o v + \nu \nabla u_o \cdot \nabla v)dx = \int_\Omega \tilde{f} v dx, \ \forall v \in V; \end{cases}$$

problem (2.12) has a unique solution.

Substracting now (2.12) from (2.4), we observe that $u_\lambda = \tilde{u} - u_o$, which implies in turn that

$$(2.13) \qquad A\lambda = (\tilde{u} - u_o)|\gamma = g - u_o|\gamma.$$

We have thus proved (2.8) for $\beta = g - u_0|_\gamma$. □

The multiplier λ is therefore the solution of the linear variational problem

$$(2.14) \qquad \begin{cases} \lambda \in H^{-1/2}(\gamma), \\ \\ <\mu, A\lambda> = <\mu, \beta>, \ \forall \mu \in H^{-1/2}(\gamma). \end{cases}$$

Operator A is definitely close to those *Steklov-Poincaré* operators which play a very important role in the theory of domain decomposition methods.

From the properties of A we can solve problem (2.8), (2.14) by a conjugate gradient algorithm operating in the space $H^{-1/2}(\gamma)$. Indeed, due to the difficulties associated to the handling of space $H^{-1/2}(\gamma)$ we shall consider the solution of (2.8), (2.14) in the space $L^2(\gamma)$. This simplification makes sense if $\lambda \in L^2(\lambda)$; since λ is essentially the jump of $\frac{\partial \tilde{u}}{\partial n}$ at γ, λ will be in $L^2(\gamma)$ if g is sufficiently smooth ($g \in H^s(\gamma)$, $s \geq 1$, will imply this property).

Description of the conjugate gradient algorithm:

If the solution λ of (2.8), (2.14) is in $L^2(\gamma)$, it clearly satisfies

$$(2.15) \qquad \begin{cases} \lambda \in L^2(\gamma), \\ \\ \int_\gamma (A\lambda)\mu d\gamma = \int_\gamma \beta \mu d\gamma, \ \forall \mu \in L^2(\gamma), \end{cases}$$

with $\beta = g - u_0|_\gamma$. Applying to the linear variational problem (2.15) the general conjugate gradient algorithm described in, e.g., [6, Chapter 3], we obtain

$$(2.16) \qquad \lambda^0 \in L^2(\gamma) \ \textit{given};$$

solve

$$\text{(2.17)}\qquad \begin{cases} u^o \in V, \\ \displaystyle\int_\Omega (\alpha u^o v + \nu \nabla u^o \cdot \nabla v)dx = \int_\Omega \tilde{f} v dx + \int_\gamma \lambda^o v d\gamma, \ \forall v \in V, \end{cases}$$

and then

$$\text{(2.18)}\qquad \begin{cases} g^o \in L^2(\gamma), \\ \displaystyle\int_\gamma g^o \mu d\gamma = \int_\gamma (u^o - g)\mu d\gamma, \ \forall \mu \in L^2(\gamma), \end{cases}$$

and set

$$\text{(2.19)}\qquad w^o = g^o. \quad \square$$

For $n \geq 0$, *assuming that* λ^n, g^n, w^n *are known, compute* λ^{n+1}, g^{n+1}, w^{n+1}, *as follows:*

Solve

$$\text{(2.20)}\qquad \begin{cases} \overline{u}^n \in V, \\ \displaystyle\int_\Omega (\alpha \overline{u}^n v + \nu \nabla \overline{u}^n \cdot \nabla v)dx = \int_\gamma w^n v d\gamma, \ \forall v \in V, \end{cases}$$

compute

$$\text{(2.21)}\qquad \rho_n = \frac{\displaystyle\int_\gamma |g^n|^2 d\gamma}{\displaystyle\int_\gamma \overline{u}^n w^n d\gamma},$$

set

$$\text{(2.22)}\qquad \lambda^{n+1} = \lambda^n - \rho_n w^n,$$

$$\text{(2.23)}\qquad u^{n+1} = u^n - \rho_n \overline{u}^n,$$

and solve

$$(2.24)\qquad \begin{cases} g^{n+1}\in L^2(\gamma), \\ \displaystyle\int_{\tilde\gamma} g^{n+1}\mu d\gamma = \int_{\tilde\gamma} g^n\mu d\gamma - \rho_n\int_{\tilde\gamma}\bar u^n\mu d\gamma,\ \forall\mu\in L^2(\gamma). \end{cases}$$

If $\|g^{n+1}\|_{L^2(\gamma)}\Big/\|g^o\|_{L^2(\gamma)}\leq\epsilon$, *take* $\lambda=\lambda^{n+1}$ *and* $\tilde u = u^{n+1}$; *if not compute*

$$(2.25)\qquad \gamma_n = \|g^{n+1}\|^2_{L^2(\gamma)}\Big/\|g^n\|^2_{L^2(\gamma)}$$

and set

$$(2.26)\qquad w^{n+1} = g^{n+1} + \gamma_n w^n.$$

Do n=n+1 *and go to* (2.20).

Remark 2.2: It follows from (2.16) – (2.26) that the effect of the actual geometry is taking place in

(i) The way $\tilde f$ is constructed

(ii) The integrals over γ in the right hand sides of (2.17) and (2.20)

(iii) Evaluation of the $L^2(\gamma)$-scalar products in (2.18), (2.21), (2.24) and (2.25).

On the other hand - and this is a justification of the method - the bilinear form in (2.17), (2.20) is independent of ω and γ.

In the following Section 2.4, we shall discuss a finite element implementation of problem (2.4), (2.5) and of the conjugate gradient algorithm (2.16)–(2.26).

2.4 Finite Element Approximation of Problem (2.4), (2.5).

Let V_h (resp. Λ_h) be a finite dimensional subspace of $V=H_o^1(\Omega)$ (resp. of $L^2(\gamma)$). We approximate the variational system (2.4), (2.5) by

$$\int_\Omega (\alpha u_h v_h + \nu \nabla u_h \cdot \nabla v_h) dx = \int_\Omega \tilde{f} v_h dx + \int_\gamma \lambda_h v_h d\gamma, \ \forall v_h \in V_h, \tag{2.27}$$

$$\int_\gamma (u_h - g_h)\mu_h d\gamma = 0, \ \forall \mu_h \in \Lambda_h, \tag{2.28}$$

$$u_h \in V_h, \ \lambda_h \in \Lambda_h. \tag{2.29}$$

The spaces V_h and Λ_h can be fairly independent from each other (as already observed in [7] in a related context); actually, V_h can be a *finite element space* based on a regular mesh in Ω (V_h can also be related to spectral type approximations). On the other hand Λ_h can be directly related to the geometry of γ and does not need to be satisfying uniform discretization properties. At that stage, we think that it is important to remember that Λ_h plays the role of not only $L^2(\gamma)$ but also of $H^{-1/2}(\gamma)$, which is the natural functional space for the multiplier λ. From this observation it makes sense to use a space Λ_h consisting of discontinuous functions over γ (piecewise polynomial, for example). Another important issue is the ability to compute easily boundary integrals such as

$$\int_\gamma v_h \mu_h d\gamma, \ \forall v_h \in V_h, \ \mu_h \in \Lambda_h; \tag{2.30}$$

numerical integration can be used for this purpose. Concerning the conjugate gradient algorithm (2.16)–(2.26), very few modifications have to take place to obtain its discrete equivalent, the essential ones being

$$\begin{cases} g_h^o \in \Lambda_h \\ \displaystyle\int_\gamma g_h^o \mu_h d\gamma = \int_\gamma (u_h^o - g_h)\mu_h d\gamma, \ \forall \mu_h \in \Lambda_h, \end{cases} \tag{2.31}$$

instead of (2.18), and then

$$(2.32)\qquad \begin{cases} g_h^{n+1} \in \Lambda_h, \\ \displaystyle\int_\gamma g_h^{n+1}\mu_h d\gamma = \int_\gamma g_h^n \mu_h d\gamma - \rho_n \int_\gamma \overline{u}_h^n \mu_h d\gamma, \ \forall \mu_h \in \Lambda_h, \end{cases}$$

instead of (2.24).

Numerical implementations of the above methodology will be described in the followir Section 2.5.

2.5 Numerical Experiments.

The goal of this section is to validate the fictitious domain/Lagrange multiplier paradigm through the solution of some quite simple test problems of Dirichlet type; application to the solution fo more complicated problems will be addressed in Section 3 (Navier-Stokes equations) and 4 (Helmholtz equations).

2.5.1 A first test problem.

The test problem to be discussed in this paragraph is the Dirichlet problem below

$$(2.33)\qquad \begin{cases} \alpha u - \nu \Delta u = f \ in \ \omega, \\ u = g \ on \ \gamma, \end{cases}$$

with α=100, ν=.1 and ω=(.25, .75)×(.25, .75).

The data f and g have been chosen so that the solution of problem (2.33) is

$$u(x_1, x_2) = x_1^2 + x_2^2, \ \forall \ \{x_1, x_2\} \in \omega,$$

(which implies $f(x_1, x_2) = \alpha(x_1^2 + x_2^2) - 4\nu$).

In order to test our fictitious domain methodology, domain ω has been imbedded in the larger

domain $\Omega=(0,1) \times (0,1)$ (as shown in Figure 2.2, below)

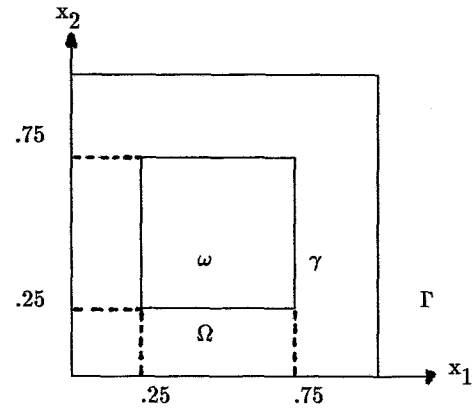

Figure 2.2

and function f has been extended by $\alpha(x_1^2+x_2^2)-4\nu$ over Ω.

For the space V occurring in (2.4) (see Section 2.2) we have taken

$$V = H_P^1(\Omega) = \{v|v\in H^1(\Omega),\ v \textit{ periodic at } \Gamma\}.$$

In order to implement the fictitious domain methodology we introduced triangulations $\mathcal{T}_h$ of Ω such that the one shown in Figure 2.3

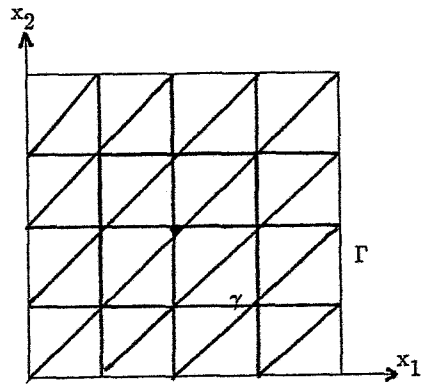

Figure 2.3 (Triangulation of Ω; $h=1/4$).

These triangulations are such that γ is supported by edges of $\mathcal{T}_h$. Next we approximate V by V_h such that

$$V_h = \left\{v_h | v_h \in V \cap C^0(\bar{\Omega}),\ v_h|_T \in P_1,\ \forall T \in \mathcal{T}_h\right\},$$

with P_1: space of the polynomials in 2 variables of degree ≤ 1. In order to use the discrete formulation (2.27)–(2.29) (see Section 2.4) we need to define the multiplier space Λ_h; an obvious choice is to define Λ_h by

$$\Lambda_h = \left\{\mu_h | \mu_h = \tilde{\mu}_h|_\gamma,\ \tilde{\mu}_h \in V_h\right\}; \tag{2.34}$$

another natural choice is to define Λ_h by

$$\Lambda_h = \left\{\mu_h | \mu_h,\ \mu_h = \text{const. } \textit{on the edges of } \mathcal{T}_h \textit{ supported by } \gamma\right\}. \tag{2.35}$$

Indeed choices (2.34), (2.35) lead to satisfactory results (second order accuracy is obtained), but results of much better quality (although no better than second order accurate) are obtained if one defines Λ_h by

$$\begin{cases} \Lambda_h = \left\{\mu_h | \mu_h = \text{const. } \textit{on the intervals joining the midpoints of the edges of} \right. \\ \left. \mathcal{T}_h \textit{ supported by } \gamma\right\}; \end{cases} \tag{2.36}$$

choice (2.36) is visualized on Figure 2.4 below (we have shown the midpoints).

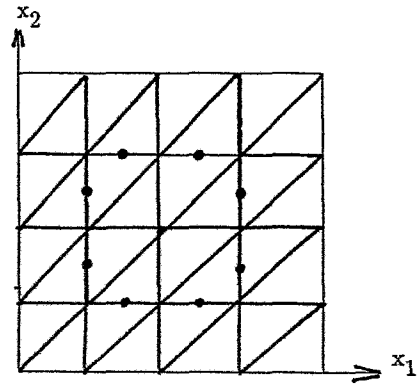

Figure 2.4

In a sense we use a *staggered* boundary grid to define Λ_h by (2.36). When implementing the finite dimensional version of algorithm (2.16)−(2.26) the discrete analogues of problems (2.17), (2.20) have been solved by a *Fast Elliptic Solver* compatible with periodic boundary conditions and based on *cyclic reduction* (see [2], [8]−[14] and the references therein for this approach). Table 2.1, below, shows the performance of the finite element analogue of algorithm (2.16)−(2.26) applied to the test problem considered here, when Λ_h is defined by (2.36) (the stopping criterion is the discrete analogue of

$$\int_\gamma |g^{n+1}|^2 d\gamma \Big/ \int_\gamma |g^o|^2 d\gamma \leq 10^{-14}). \tag{2.37}$$

h	Number of iterations	$\|u-u_h\|_\infty$
1/8	7	2.6×10^{-3}
1/16	13	6.5×10^{-4}
1/32	20	1.6×10^{-4}
1/64	27	4.1×10^{-5}

Table 2.1

The above table clearly suggests that:

(i) The approximation is *second order accurate.*

(ii) The number of iterations increases as $h^{-1/2}$, which is what we can expect from a theoretical point of view since the condition number of the discrete analogue of operator A (see Section 2.3) is $O(h^{-1})$.

Figure 2.5 shows (on a logarithmic scale) the variation of the residual $\|g_h^{n+1}\|_{L^2(\gamma)} \Big/ \|g_h^0\|_{L^2(\gamma)}$ versus the number of iterations, for h=1/64. The computed results coincide quite well with the exact ones as shown on Figure 2.6 where the variations of $x_1 \longrightarrow u(x_1,.5)$ and $x_1 \longrightarrow u_h(x_1, .5)$ have been represented; both curves can not be distinguished, in practice. Actually, and as it can be expected, the maximum error is reached on γ (see Table 2.2).

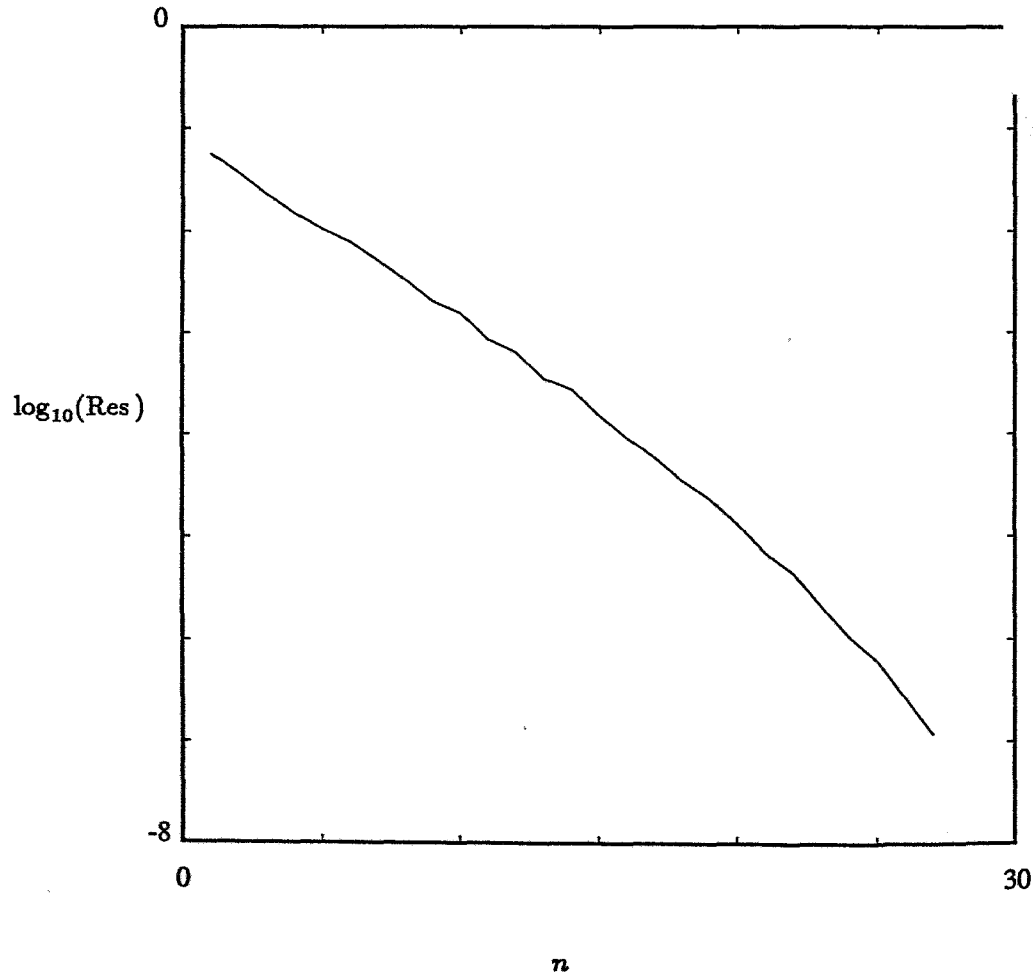

Figure 2.5

Figure 2.5 shows (on a logarithmic scale) the variation of the residual $\|g_h^{n+1}\|_{L^2(\gamma)} / \|g_h^o\|_{L^2(\gamma)}$ versus the number of iterations, for h=1/64. The computed results coincide quite well with the exact ones as shown on Figure 2.6 where the variations of $x_1 \longrightarrow u(x_1,.5)$ and $x_1 \longrightarrow u_h(x_1, .5)$ have been represented; both curves can not be distinguished, in practice. Actually, and as it can be expected, the maximum error is reached on γ (see Table 2.2).

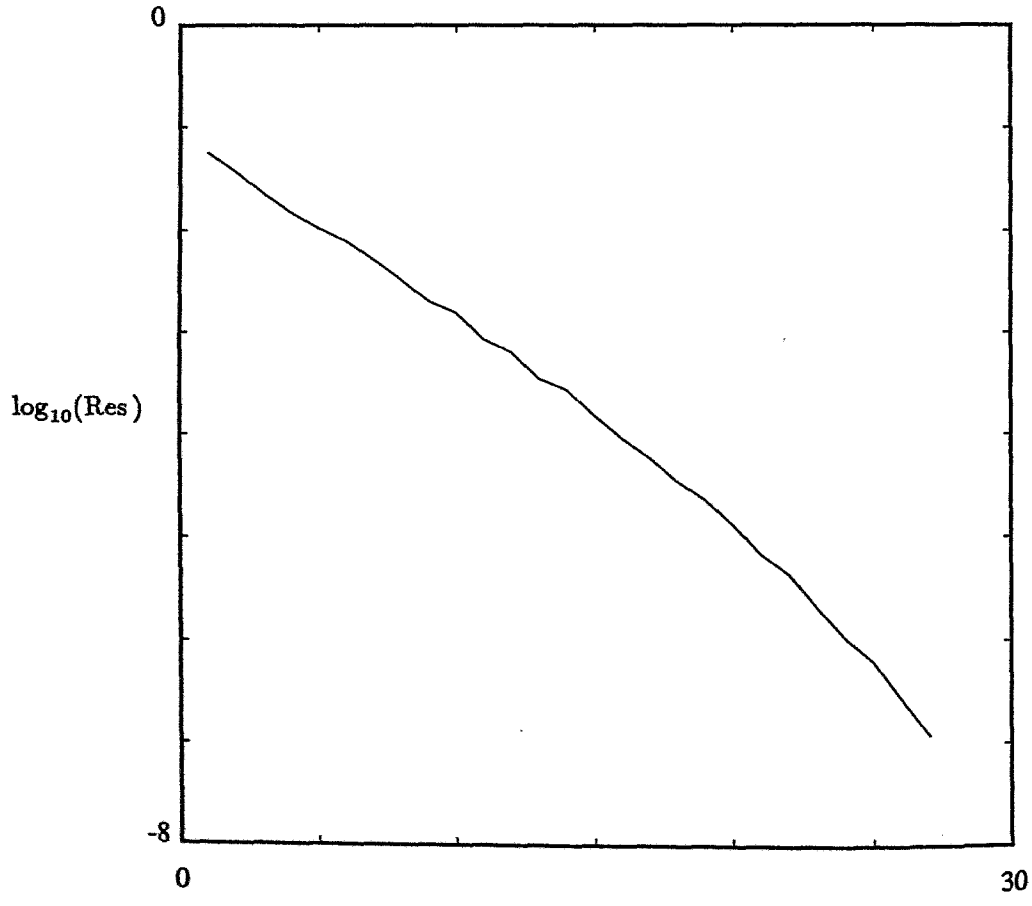

Figure 2.5

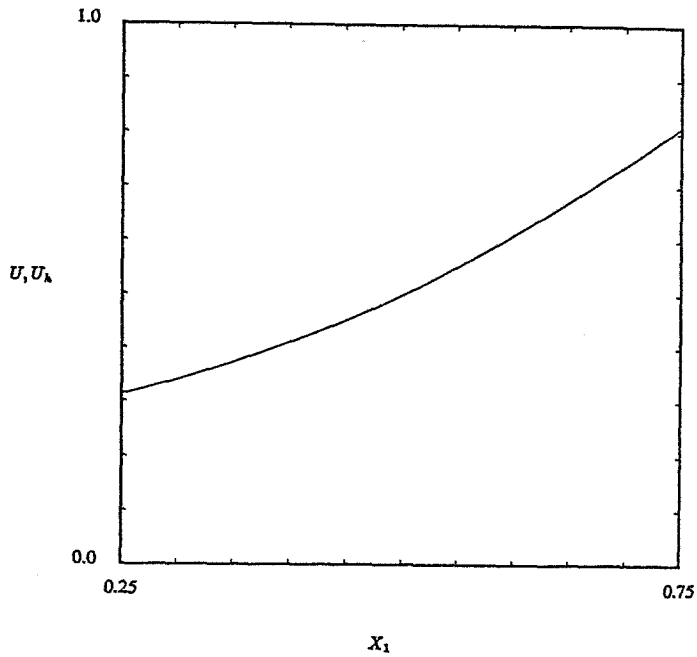

Figure 2.6

x_1	x_2	Approximated Solution	Error
0.25000000E+00	0.50000000E+00	0.31245938E+00	0.40619671E-04
0.26562500E+00	0.50000000E+00	0.32053171E+00	0.24931408E-04
0.28125000E+00	0.50000000E+00	0.32908626E+00	0.15297547E-04
0.29687500E+00	0.50000000E+00	0.33812538E+00	0.93880402E-05
0.31250000E+00	0.50000000E+00	0.34765049E+00	0.57648498E-05
0.32812500E+00	0.50000000E+00	0.35766247E+00	0.35440663E-05
0.34375000E+00	0.50000000E+00	0.36816188E+00	0.21831863E-05
0.35937500E+00	0.50000000E+00	0.37914904E+00	0.13494521E-05
0.37500000E+00	0.50000000E+00	0.39062416E+00	0.83882777E-06
0.39062500E+00	0.50000000E+00	0.40258736E+00	0.52624221E-06
0.40625000E+00	0.50000000E+00	0.41503873E+00	0.33506095E-06
0.42187500E+00	0.50000000E+00	0.42797830E+00	0.21836723E-06
0.43750000E+00	0.50000000E+00	0.44140610E+00	0.14749417E-06
0.45312500E+00	0.50000000E+00	0.45532216E+00	0.10501266E-06
0.46875000E+00	0.50000000E+00	0.46972648E+00	0.80464828E-07
0.48437500E+00	0.50000000E+00	0.48461907E+00	0.67802001E-07
0.50000000E+00	0.50000000E+00	0.49999994E+00	0.63901782E-07
0.51562500E+00	0.50000000E+00	0.51586907E+00	0.67802073E-07
0.53125000E+00	0.50000000E+00	0.53222648E+00	0.80464995E-07
0.54687500E+00	0.50000000E+00	0.54907216E+00	0.10501299E-06
0.56250000E+00	0.50000000E+00	0.56640610E+00	0.14749484E-06
0.57812500E+00	0.50000000E+00	0.58422830E+00	0.21836867E-06
0.59375000E+00	0.50000000E+00	0.60253873E+00	0.33506427E-06
0.60937500E+00	0.50000000E+00	0.62133736E+00	0.52625034E-06
0.62500000E+00	0.50000000E+00	0.64062416E+00	0.83884843E-06
0.64062500E+00	0.50000000E+00	0.66039904E+00	0.13495057E-05
0.65625000E+00	0.50000000E+00	0.68066188E+00	0.21833265E-05
0.67187500E+00	0.50000000E+00	0.70141247E+00	0.35444325E-05
0.68750000E+00	0.50000000E+00	0.72265048E+00	0.57657965E-05
0.70312500E+00	0.50000000E+00	0.74437538E+00	0.93904192E-05
0.71875000E+00	0.50000000E+00	0.76658626E+00	0.15303144E-04
0.73437500E+00	0.50000000E+00	0.78928170E+00	0.24942449E-04
0.75000000E+00	0.50000000E+00	0.81245937E+00	0.40628824E-04

Table 2.2

3. Application to the Navier-Stokes equations for Dirichlet boundary conditions.

3.1 Generalities. Formulation.

In this section we shall briefly discuss fictitious domain methods for solving the *unsteady incompressible Navier-Stokes* equations for *Dirichlet boundary conditions.* In this section, which can be seen as a generalization of [4] we take full advantage of *time discretization by operator splitting methods* to implement fictitious domain methods.

Using the notation of Figure 2.1 (see Section 2.2) we consider the following Navier-Stokes equations

$$\frac{\partial \mathbf{u}}{\partial t} - \nu \nabla^2 \mathbf{u} + (\mathbf{u}\cdot\nabla)\mathbf{u} + \nabla p = \mathbf{f} \text{ in } \omega, \tag{3.1}$$

$$\nabla\cdot\mathbf{u} = 0 \text{ in } \omega \text{ (incompressibility condition)}, \tag{3.2}$$

$$\mathbf{u} = \mathbf{g} \text{ on } \gamma \text{ (with } \int_{\gamma} \mathbf{g}\cdot\mathbf{n}\, d\gamma = 0), \tag{3.3}$$

$$\mathbf{u}(x,0) = \mathbf{u}_0(x),\ x\in\omega, \text{ with } \nabla\cdot\mathbf{u}_0 = 0. \tag{3.4}$$

In (3.1), (3.2), $\mathbf{u} = \{u_i\}_{i=1}^{d}$ is the *flow velocity*, p is the *pressure*, f is a *density of external forces*, $\nu(>0)$ is a *viscosity parameter*, $\nabla = \{\frac{\partial}{\partial x_i}\}_{i=1}^{d}$, $\nabla^2 = \Delta = \sum_{i=1}^{d} \frac{\partial^2}{\partial x_i^2}$, and

$$(\mathbf{v}\cdot\nabla)\mathbf{w} = \Big\{\sum_{j=1}^{d} v_j \frac{\partial w_i}{\partial x_j}\Big\}_{i=1}^{d}.$$

3.2 An equivalence result.

We imbed ω in Ω as shown in Figure 2.1 and define

$$V_P = \Big\{v \mid v\in(H^1(\Omega))^d,\ v \textit{ periodic} \text{ at } \Gamma\Big\}.$$

Next we observe that if U_0 is an extension of u_0 which is divergence free in Ω, and $\tilde{f}$ an extension of f, we have equivalence between (3.1)–(3.4) and

$$(3.5)\qquad \begin{cases} \displaystyle\int_\Omega \frac{\partial U}{\partial t}\cdot v dx + \nu\int_\Omega \nabla U\cdot\nabla v dx + \int_\Omega (U\cdot\nabla)U\cdot v dx - \int_\Omega P\nabla\cdot v dx = \\ \displaystyle\int_\Omega \tilde{f}\cdot v dx + \int_\gamma \lambda\cdot v d\gamma,\ \forall v\in V_P;\ U(t)\in V_P \text{ a.e. } t>0, \end{cases}$$

$$(3.6)\qquad \nabla\cdot U = 0 \text{ in } \Omega,$$

$$(3.7)\qquad U(x,0) = U_o(x),\ x\in\Omega,$$

$$(3.8)\qquad U = g \text{ on } \gamma,$$

in the sense that

$$(3.9)\qquad U|_\omega = u,\ P|_\omega = p.$$

Concerning the multiplier λ, its interpretation is very simple since it is equal to the jump of $\nu\frac{\partial U}{\partial n} - nP$ at γ.

3.3 A method combining fictitious domains and operator splitting.

In order to solve (3.5)–(3.9) we shall time discretize it by an operator splitting method like the ones discussed in e.g. [6], [15]–[18], [31], [33], [34].

For simplicity, we consider the time discretization of (3.5)–(3.9) by the Peaceman-Rachford scheme (cf. [15]). With $\Delta t(>0)$ a time discretization step we obtain

$$(3.10)\qquad U^o = U_o;$$

for $n\geq 0$, *knowing* U^n, *we compute* $\{U^{n+1/2}, P^{n+1/2}, \lambda^{n+1/2}\}$ *and then* U^{n+1} *by solving*

$$(3.11)_1 \quad \begin{cases} \int_\Omega \frac{U^{n+1/2}-U^n}{\Delta t/2}\cdot v dx + \frac{\nu}{2}\int_\Omega \nabla U^{n+1/2}\cdot\nabla v dx - \int_\Omega P^{n+1/2}\nabla\cdot v dx - \int_\gamma \lambda^{n+1/2}\cdot v d\gamma = \\ \int_\Omega f^{n+1/2}\cdot v dx - \frac{\nu}{2}\int_\Omega \nabla U^n\cdot\nabla v dx - \int_\Omega (U^n\cdot\nabla)U^n\cdot v dx, \ \forall v\in V_P, \end{cases}$$

$$(3.11)_2 \quad \nabla\cdot U^{n+1/2} = 0 \text{ in } \Omega,$$

$$(3.11)_3 \quad U^{n+1/2} = g^{n+1/2} \text{ on } \gamma,$$

$$(3.11)_4 \quad U^{n+1/2}\in V_P,\ P^{n+1/2}\in L^2(\Omega),$$

and then

$$(3.12)_1 \quad \begin{cases} \int_\Omega \frac{U^{n+1}-U^{n+1/2}}{\Delta t/2}\cdot v dx + \frac{\nu}{2}\int_\Omega \nabla U^{n+1}\cdot\nabla v dx + \int_\Omega (U^{n+1/2}\cdot\nabla)U^{n+1}\cdot v dx = \\ \int_\Omega f^{n+1}\cdot v dx + \int_\gamma \lambda^{n+1/2}\cdot v d\gamma + \int_\Omega P^{n+1/2}\nabla\cdot v dx - \frac{\nu}{2}\int_\Omega \nabla U^{n+1/2}\cdot\nabla v dx, \ \forall v\in V_P, \end{cases}$$

$$(3.12)_2 \quad U^{n+1}\in V_P.$$

Due to page limitation we shall not give a detailed account on the solution of problems (3.11) and (3.12); we shall make however the following remarks:

Remark 3.1: Problem (3.11) can be solved by a variant of the algorithm described in Section 2, the main difference being that at each iteration, we have to solve a Stokes problem instead of a simple elliptic problem. However due to the periodic boundary conditions, it follows from, e.g. [18], [19], that Stokes problems can be solved by iterative techniques converging in *one iteration*

Remark 3.2: We have taken advantage of the splitting to treat the advection without being concerned about the constraint $u=g$ at γ. Also due to the periodic boundary conditions, problem (3.12) is well suited to solution methods based on high order upwinding on regular meshes, or on the backward method of characteristics (see, e.g. [20]).

Remark 3.3: The fictitious domain approach discussed here seems to be well suited for those situations where γ is *time dependent* like in some free boundary problems for example.

3.4 Numerical Experiments.

The results presented here are quite preliminary; they concern the time dependent Stokes problem

$$\frac{\partial \mathbf{u}}{\partial t} - \nu\nabla^2\mathbf{u} + \nabla p = 0 \text{ in } \omega, \tag{3.13}$$

$$\nabla\cdot\mathbf{u} = 0 \text{ in } \omega, \tag{3.14}$$

$$\mathbf{u}_0 = 0 \text{ in } \omega, \tag{3.15}$$

$$\mathbf{u} = \mathbf{g} \text{ on } \gamma, \tag{3.16}$$

in the case where $\omega=(.25, .75)\times(.25, .75)$ and where $\mathbf{g}$ is defined as follows:

$$\mathbf{g}(x,t) = (1-e^{-\alpha t})\ \{1,0\} \text{ if } x_1\in(.25, .75),\ x_2= .75;\ \mathbf{g} = 0 \text{ elsewhere on } \gamma. \tag{3.17}$$

On the basis of [18], we have taken the same triangulation to define the discrete velocity and pressure spaces, this being justified by the periodic boundary conditions. It seems however that the space Λ_h containing the discrete multipliers has to be properly defined in order to avoid spurious oscillations for the pressure; we shall go back on this fundamental issue in a forthcoming article.

Via time discretization, problem (3.13)−(3.17) has been reduced to a sequence of Stokes problems, which were solved by a fictitious domain method closely related to the one discussed in Section 2 for elliptic problems. Integration has been carried out until a steady state has been reached. We have taken $\nu=10^{-2}$, $\alpha=50$, $\Delta t=10^{-2}$ and $h=1/32$. The various elliptic problems encountered in the solution process have been solved by *cyclic reduction* as in Section 2.

Figure 3.1 shows the streamlines of the computed solution in ω. Figure 3.2 shows the graph of the computed stream function ψ, i.e., the solution of the discrete analogue of

$$-\Delta\psi = \frac{\partial u_2}{\partial x_1} - \frac{\partial u_1}{\partial x_2} \text{ in } \omega,\ \psi = 0 \text{ on } \gamma.$$

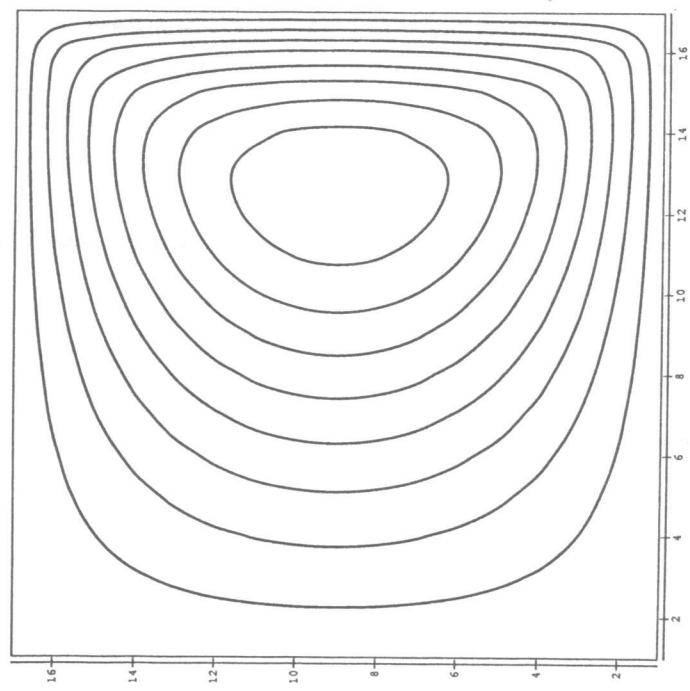

Figure 3.1

(Streamlines of the steady solution)

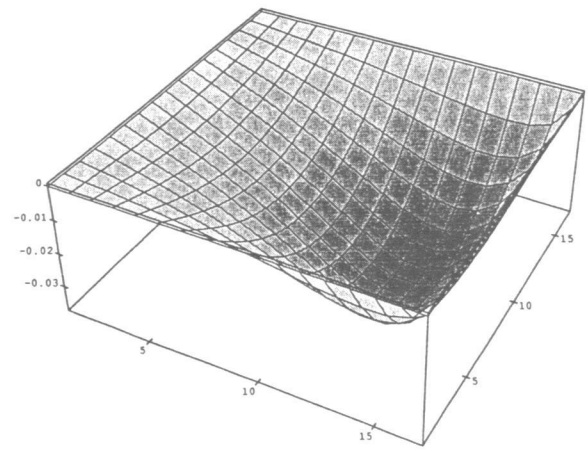

Figure 3.2

(Stream function visualization)

Figures 3.3 and 3.4 show the discrete pressure contours (isobar lines) and graph, respectively. We observe that the discrete pressure is totally clean of spurious oscillations, despite the fact that the same triangulation has been used to approximate both pressure and velocity.

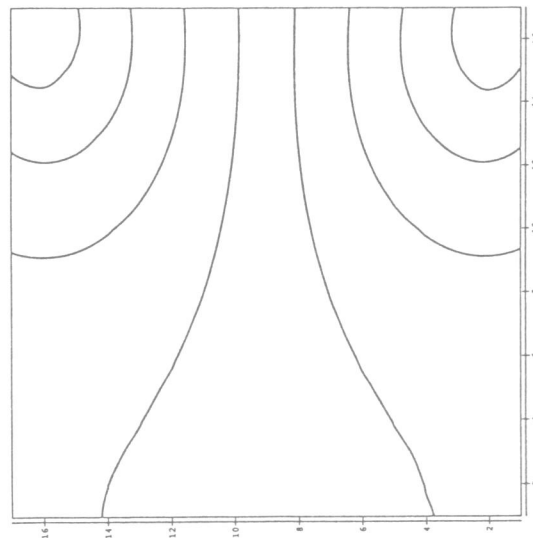

Figure 3.3
(Pressure contours)

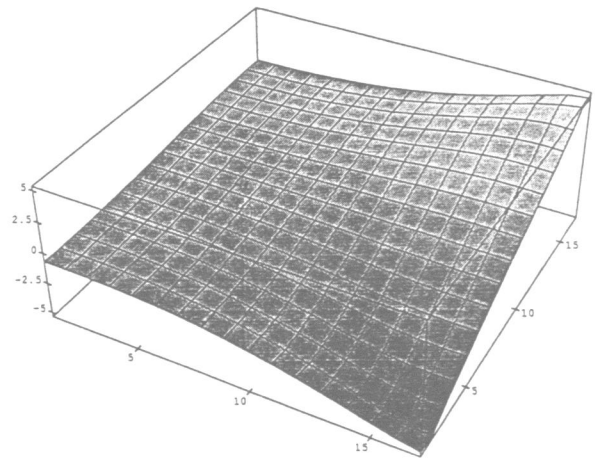

Figure 3.4
(Pressure visualization)

4. Lagrange multiplier/fictitious domain solution of the Helmholtz equation.

4.1 Generalities.

Motivated by Accoustics and Electromagnetics we consider the scattering of a *monochromatic wave* (of wave number k) by an obstacle $A(\subset \mathbf{R}^d$, d=2 or 3) of boundary γ. The reflected field satisfies the following *Helmholtz equation* (which is *complex* valued)

$$\Delta u + k^2 u = 0 \quad in\ \mathbf{R}^d \backslash \overline{A}, \tag{4.1}$$

$$u = g \quad on\ \gamma, \tag{4.2}$$

$$\lim_{r \to +\infty} \left(\frac{\partial}{\partial r} - ik\right) u = 0\left(r^{\frac{1-d}{2}}\right), \tag{4.3}$$

where relation (4.3) is the classical *Sommerfeld radiation condition* (see [21]). A classical approach for field solution methods is to bound $\mathbf{R}^d \backslash \overline{A}$ (see Figure 4.1) and to specifiy on the *artificial* boundary Γ well chosen absorbing boundary conditions (see, e. g., [22], [23], [24] for more details). We shall call ω the bounded physical domain and define Ω by Ω=interior of $(\overline{\omega} \cup \overline{A})$.

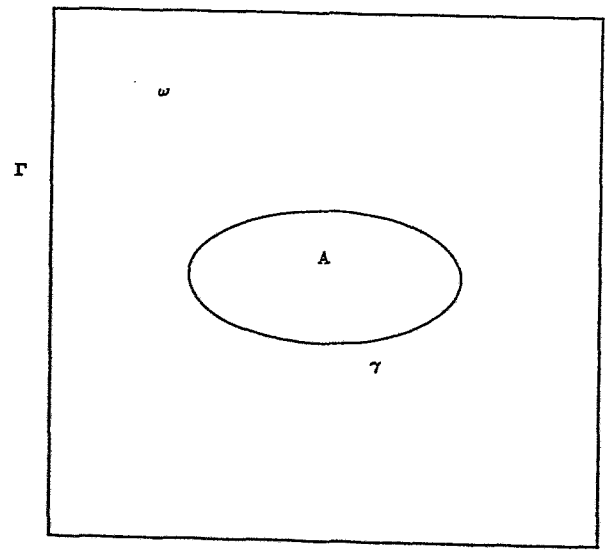

Figure 4.1

First order (resp. *second order*) absorbing boundary conditions are given by

$$\left(\frac{\partial}{\partial n} - ik\right)u = 0 \quad on\ \Gamma \tag{4.4}$$

(resp.

$$\left(\frac{\partial}{\partial n} - ik - \frac{i}{2k}\Delta_\Gamma\right)u = 0 \quad on\ \Gamma). \tag{4.5}$$

In (4.5), Δ_Γ is the *Laplace-Beltrami* operator. The Helmholtz problem whose solution will be discussed in the following paragraphs is finally (4.1), (taking place in ω), (4.2), completed by either (4.4) or (4.5). Let us mention that equations (4.1), (4.2) model electro-magnetic phenomena in the case of TM polarization (TM: Transverse Magnetic). Let us mention also that everything else being the same, the second order condition (4.5) allows smaller domains Ω, resulting therefore in significant CPU and storage savings.

A multiplier fictitious domain formulation of problems (4.1), (4.2), (4.4) and (4.1), (4.2), (4.5).

In ref. [4] a *non multiplier*/fictitious domain method (based on a *control* formulation) has been discussed and the corresponding numerical results have been reported in [25]. In this section we would like to address the solution of (4.1), (4.2), (4.5) (which is the more complicated problem) by a method which is conceptually close to the method already discussed in Section 1. Before describing the fictitious domain method it is most useful to derive an appropriate *variational formulation* of problem (4.1), (4.2), (4.5). As in [4] we introduce the following (complex) Hilbert space

$$V = \{v | v = v_1 + iv_2 \in H^1(\Omega),\ \nabla_\Gamma v \in L^2(\Gamma)\}, \tag{4.6}$$

where ∇_Γ is the *tangential gradient* of v on Γ. It is then quite easy to show that (4.1), (4.2), (4.5) is equivalent to the following variational system

$$\int_\Omega (\nabla \tilde{u}\cdot\nabla v - k^2\tilde{u}\, v)dx - i\int_\Gamma (k\tilde{u}v - \frac{1}{2k}\nabla_\Gamma \tilde{u}\cdot\nabla_\Gamma v)d\Gamma = <\lambda, v>,\ \forall \in V, \tag{4.7}$$

$$(4.8)\qquad <\mu, \tilde{u}-g>=0,\ \forall \mu \in H^{-\frac{1}{2}}(\gamma),$$

$$(4.9)\qquad \tilde{u}\in V,\ \lambda \in H^{-1/2}(\gamma).$$

In (4.7), (4.8), $<\cdot, \cdot>$ denotes the duality pairing between $H^{-\frac{1}{2}}(\gamma)$ and $H^{\frac{1}{2}}(\gamma)$. We clearly have $u=\tilde{u}|_{\omega}$. From now on, we shall drop the $\tilde{}$ from $\tilde{u}$. Despite the fact that computers can work in complex arithmetic we shall consider (4.7)-(4.9) as a system of real valued equations for the unknown functions u_1, u_2, such that $u=u_1+iu_2$, and λ_1, λ_2 such that $\lambda=\lambda_1+i\lambda_2$. We shall denote by u and λ the pairs $\{u_1, u_2\}$ and $\{\lambda_1, \lambda_2\}$, respectively. With this notation, equations (4.7)−(4.9) yield (with this time V defined over $\mathbb{R}$)

$$(4.10)\qquad \begin{cases} u\in V\times V;\ \forall v\in V\times V \textit{ we have} \\ \int_{\Omega} (\nabla u\cdot\nabla v - k^2 u\cdot v)dx + \int_{\Gamma} (kRu\cdot v - \frac{1}{2k}\nabla_{\Gamma}Ru\cdot\nabla_{\Gamma}v)d\Gamma = <\lambda, v>, \end{cases}$$

$$(4.11)\qquad <\mu, u-g> = 0,\ \forall \mu \in H^{-1/2}(\gamma)\times H^{-1/2}(\gamma),$$

where, in (4.10), the (rotation) matrix R is given by

$$(4.12)\qquad R = \begin{pmatrix} 0 & 1 \\ -1 & 0 \end{pmatrix},$$

and where $g = \{g_1, g_2\}$ (if $g=g_1+ig_2$).

4.3 Iterative solution of Problem (4.10), (4.11).

4.3.1 Generalities.

Due to the presence of matrix R, the bilinear form in the left hand side of the equation in (4.10) is *nonsymmetric*; indeed it is also *indefinite*. Due to these properties, we can not expect algorithms like (2.16)−(2.26) (which is essentially a saddle-point searcher (à la Uzawa; cf. [26, Chapter 2 and Appendix 2])) to converge. Unfortunately, numerical experiments confirm this

prediction. Since this preliminary article is mainly a *feasibility study*, we have decided to address the solution by a least-squares/conjugate gradient algorithm; indeed the resulting formulation and associated algorithm remind strongly of the fictitious domain/control approach discussed in [4] and suggested to us by P. L. Lions [27]. We intend to address subsequently the solution of (4.10), (4.11) by more sophisticated algorithms (like those discussed in [28], for example).

4.3.2 A least-squares Formulation of Problem (4.10), (4.11).

Following an approach which has been successful in other contexts (as shown in [29]—[34], for example) we formulate problem (4.10), (4.11) by

$$\text{(4.13)} \qquad \operatorname*{Min}_{\{v,\mu\}\in V\times V\times\Lambda} J(v,\mu),$$

where $\Lambda = L^2(\gamma)\times L^2(\gamma)$, where $J: V\times V\times\Lambda \longrightarrow \mathbb{R}$ is defined (with α and β both positive) by

$$\text{(4.14)} \qquad J(v,\mu) = \frac{1}{2}\int_\Omega (|\nabla y|^2 + \alpha|y|^2)dx + \frac{\beta}{2}\int_\gamma |\eta|^2 d\gamma,$$

with $y(=y(v,\mu))$ and $\eta(=\eta(v,\mu))$ the respective solutions of

$$\text{(4.15)} \qquad \begin{cases} y\in V\times V;\ \forall z\in V\times V \text{ we have } \displaystyle\int_\Omega (\nabla y\cdot\nabla z + \alpha y\cdot z)dx = \\ \displaystyle\int_\Omega (\nabla v\cdot\nabla z - k^2 v\cdot z)dx + \int_\Gamma (kRv\cdot z - \frac{1}{2k}\nabla_\Gamma Rv\cdot\nabla_\Gamma z)d\Gamma - \int_\Gamma \mu\cdot z d\gamma, \end{cases}$$

$$\text{(4.16)} \qquad \eta\in\Lambda;\ \forall\theta\in\Lambda \text{ we have } \int_\gamma \eta\cdot\theta d\gamma = \int_\gamma (v-g)\cdot\theta d\gamma.$$

4.3.3 Conjugate Gradient Solution of the Least Squares Problem (4.13).

Using a classical *perturbation analysis* we should easily prove that the *derivative* $J'(v,\mu)$ of $J(\cdot,\cdot)$ at $\{v,\mu\}$ is defined by

$$(4.17)\qquad \begin{cases} <J'(v,\mu),\{w,\theta\}> = \displaystyle\int_\Omega (\nabla y\cdot\nabla w - k^2 y\cdot w)dx + \int_\Gamma (kR^t y\cdot w + \frac{1}{2k}\nabla_\Gamma R^t y\cdot\nabla_\Gamma w)d\Gamma \\ + \beta\displaystyle\int_\gamma \eta\cdot w d\gamma - \int_\gamma y\cdot\theta d\gamma,\ \forall\{w,\theta\}\in V\times V\times\Lambda. \end{cases}$$

Using now the knowledge of J' we can solve problem (4.13) by the following conjugate gradi algorithm which operates on $V\times V\times\Lambda$ equipped with the following metric

$$\|\{z,\theta\}\|_{V\times V\times\Lambda} = \Big(\int_\Omega (|\nabla z|^2 + \alpha|z|^2)dx + \beta\int_\gamma |\theta|^2 d\gamma\Big)^{\frac{1}{2}}.$$

Initialization:

$$(4.18)\qquad \{u^o,\lambda^o\}\in V\times V\times\Lambda \text{ is given;}$$

solve then the following variational system

$$(4.19)\qquad \begin{cases} y^o\in V\times V;\ \forall z\in V\times V, \text{ we have } \displaystyle\int_\Omega (\nabla y^o\cdot\nabla z + \alpha y^o\cdot z)dx = \\ \displaystyle\int_\Omega (\nabla u^o\cdot\nabla z - k^2 u^o\cdot z)dx + \int_\Gamma (kRu^o\cdot z - \frac{1}{2k}\nabla_\Gamma Ru^o\cdot\nabla_\Gamma z)d\Gamma - \int_\gamma \lambda^o\cdot z d\gamma, \end{cases}$$

$$(4.20)\qquad \eta^o\in\Lambda;\ \forall\theta\in\Lambda \text{ we have } \int_\gamma \eta^o\cdot\theta d\gamma = \int_\gamma (u^o - g)\cdot\theta d\gamma.$$

Next, define $g^o = \{g_u^o, g_\lambda^o\}\in V\times V\times\Lambda$ *by*

$$(4.21)\qquad \begin{cases} \displaystyle\int_\Omega (\nabla g_u^o\cdot\nabla z + \alpha g_u^o\cdot z)dx = \int_\Omega (\nabla y^o\cdot\nabla z - k^2 y^o\cdot z)dx + \int_\Gamma (kR^t y\cdot z - \frac{1}{2k}\nabla_\Gamma R^t y^o\cdot\nabla_\Gamma z)d\Gamma \\ + \beta\displaystyle\int_\gamma \eta^o\cdot z d\gamma,\ \forall z\in V\times V;\ g_u^o\in V\times V, \end{cases}$$

$$(4.22)\qquad \begin{cases} \beta\displaystyle\int_\gamma g_\lambda^o\cdot\mu d\gamma = -\int_\gamma y^o\cdot\mu d\gamma,\ \forall\mu\in\Lambda, \\ g_\lambda^o\in\Lambda, \end{cases}$$

and set

$$w^o \left(= \{w_u^o, w_\lambda^o\}\right) = \{g_u^o, g_\lambda^o\}. \quad \square \tag{4.23}$$

Then for $n \geq 0$, *assuming that* u^n, λ^n, g^n, w^n *are known, we update them as follows:*

Descent:

Solve

$$\begin{cases} \overline{y}^n \in V \times V;\ \forall z \in V \times V \text{ we have } \displaystyle\int_\Omega (\nabla \overline{y}^n \cdot \nabla z + \alpha \overline{y}^n \cdot z)dx = \\ \displaystyle\int_\Omega (\nabla w_u^n \cdot \nabla z - k^2 w_u^n \cdot z)dx + \int_\Gamma (kRw_u^n \cdot z - \frac{1}{2k} \nabla_\Gamma Rw_u^n \cdot \nabla_\Gamma z)d\Gamma - \int_\gamma w_\lambda^n \cdot z d\gamma, \end{cases} \tag{4.24}$$

$$\overline{\eta}^n \in \Lambda;\ \forall \theta \in \Lambda \text{ we have } \int_\gamma \overline{\eta}^n \cdot \theta d\gamma = \int_\gamma w_u^n \cdot \theta d\gamma, \tag{4.25}$$

and then

$$\begin{cases} \overline{g}_u^n \in V \times V;\ \forall z \in V \times V \text{ we have } \displaystyle\int_\Omega (\nabla \overline{g}_u^n \cdot \nabla z + \alpha \overline{g}_u^n \cdot z)dx = \\ \displaystyle\int_\Omega (\nabla \overline{y}^n \cdot \nabla z - k^2 \overline{y}^n \cdot z)dx + \int_\Gamma (kR^t \overline{y}^n \cdot z - \frac{1}{2k} \nabla_\Gamma R^t \overline{y}^n \cdot \nabla_\Gamma z)d\Gamma + \beta \int_\gamma \overline{\eta}^n \cdot z d\gamma, \end{cases} \tag{4.26}$$

$$\overline{g}_\lambda^n \in \Lambda;\ \forall \mu \in \Lambda \text{ we have } \beta \int_\gamma \overline{g}_\lambda^n \cdot \mu d\gamma = - \int_\gamma \overline{y}^n \cdot \mu d\gamma. \tag{4.27}$$

Compute now

$$\rho_n = \frac{\displaystyle\int_\Omega \left(|\nabla g_u^n|^2 + \alpha |g_u^n|^2\right)dx + \beta \int_\gamma |g_\lambda^n|^2 d\gamma}{\displaystyle\int_\Omega \left(\nabla \overline{g}_u^n \cdot \nabla w_u^n + \alpha \overline{g}_u^n \cdot w_u^n\right)dx + \beta \int_\gamma \overline{g}_\lambda^n \cdot w_\lambda^n d\gamma}, \tag{4.28}$$

and then

$$u^{n+1} = u^n - \rho_n w_u^n,\ \lambda^{n+1} = \lambda^n - \rho_n w_\lambda^n, \tag{4.29}$$

$$g_u^{n+1} = g_u^n - \rho_n \overline{g}_u^n,\ g_\lambda^{n+1} = g_\lambda^n - \rho_n \overline{g}_\lambda^n. \tag{4.30}$$

Testing the convergence and constructing the new descent direction:

If $\|g^{n+1}\|_{V\times V\times\Lambda} \Big/ \|g^o\|_{V\times V\times\Lambda} \leq \epsilon$, *take* $u = u^{n+1}$, $\lambda = \lambda^{n+1}$; *if not compute*

$$\gamma_n = \frac{\|g^{n+1}\|^2_{V\times V\times\Lambda}}{\|g^n\|^2_{V\times V\times\Lambda}}, \tag{4.31}$$

and

$$\left\{w_u^{n+1}, w_\lambda^{n+1}\right\} = \left\{g_u^{n+1}, g_\lambda^{n+1}\right\} + \gamma_n \left\{w_u^n, w_\lambda^n\right\}. \tag{4.32}$$ □

Do $n = n+1$ *and go to* (4.24).

4.4 Finite Element Implementation of the Fictitious Domain Methodology.

In Sections 4.2 and 4.3 we have described a fictitious domain methodology for the solution of the Helmholtz equation. The finite element implementation of this methodology, and particularly of the conjugate gradient algorithm (4.18)−(4.33), obeys essentially to the rules and principles described in Section 2.4, concerning the solution of the Dirichlet problem (2.1), (2.2). This is particularly true concerning the choice of the multiplier space Λ_h and the numerical evaluation of the various boundary integrals over the *physical boundary* γ.

4.5 Numerical Experiments.

4.5.1 Generalities.

This section has to be understood essentially as a feasibility study, in order to obtain some very preliminary information concerning the possibility of solving Helmholtz and ultimately Maxwell

equations by fictitious domain methods. For example instead of Sommerfeld radiation conditions, we have been prescribing Dirichlet conditions on the exterior boundary of the physical domain. Also, as mentioned above, we have been using a (almost) brute force iterative method to compute the approximate solutions. The test problems to be discussed concern the solution of the Helmholtz equation

$$\Delta u + k^2 u = 0 \text{ in } \omega, \tag{4.33}$$

$$u = g \text{ on } \gamma \cup \Gamma, \tag{4.34}$$

where, in (4.33), (4.34), we use the notation of Figure 4.1 (See Section 4.1). The methodology is the one described in Sections 4.2, 4.3 and 4.4, in particular, the elliptic problems (of Dirichlet type) playing the role of (4.19), (4.21) and (4.24), (4.26) in algorithms (4.18)−(4.33), are solved by a Fast Dirichlet solver of cyclic reduction type. Incidently, we have taken $\alpha=0$ and $\beta=1$ in the least squares formulation (4.13). As test problems, we have considered the case where the obstacle A is a *disk* (Section 4.5.2), an *ellipse* (Section 4.5.3.), and a *double-ellipse* (Section 4.5.4).

4.5.2 A first test problem: The disk case.

For this test problem, domain A is the disk centered at {0,0} and of radius 1/4; domain Ω is the square $(-1,1)\times(-1,1)$. The Dirichlet boundary condition prescribed on γ and Γ correspond to the *exact solution*

$$u(x_1,x_2) = \sin k(x_1\cos\theta + x_2\sin\theta), \tag{4.35}$$

where, in (4.35), θ is an angle between 0 and 2π. The above function is clearly a solution of (4.33), and the angle θ controls the incidence of the plane wave hitting A. A typical mesh used for the fictitious domain calculation is shown on Figure 4.2; it corresponds to $h = 1/32$. The discrete multiplier space Λ_h is defined as in Section 2.5.2. On Figure 4.3 we have shown the variation of the discrete analogue of $\|g^n\|_{V\times\Lambda}/\|g^o\|_{V\times\Lambda}$ versus n, when using a finite dimensional variant of the conjugate gradient algorithm (4.18)−(4.32); this calculations corresponds to $\theta=\pi/4$, $k=9$ and $h=1/64$. The chaotic aspect of this curve suggests that there is plenty of room for better iterative methods and/or preconditioners. Indeed, it is worth mentioning the reorthogonalization procedure

advocated by Roux in [35], in order to reduce the effect of round -off and truncation errors on convergence of conjugate gradient algorithms.

Figures 4.4(a), (b), (c) show the variation of $\|u-u_h\|_{L^2(\Omega)}$ as a function of k for h=1, 1/32 and 1/64, respectively. We observe with interest the sudden surge in the error, occurring at tl values of k for which k^2 is an eigenvalue of the discrete negative Laplace operator on Ω, for Dirichlet boundary conditions on Γ. We also observe that these peak values decrease with h. T 4.1 displays, for k=9, and $\theta=\pi/4$, the error $\|u-u_h\|_{L^2(\omega)}$ and the number of iterations versus h.

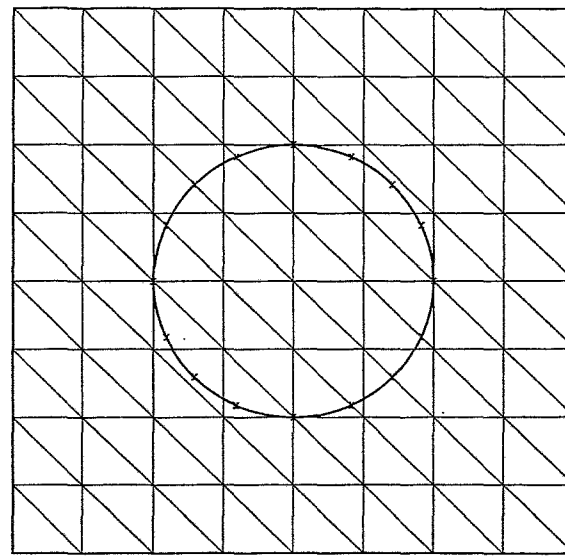

Figure 4.2

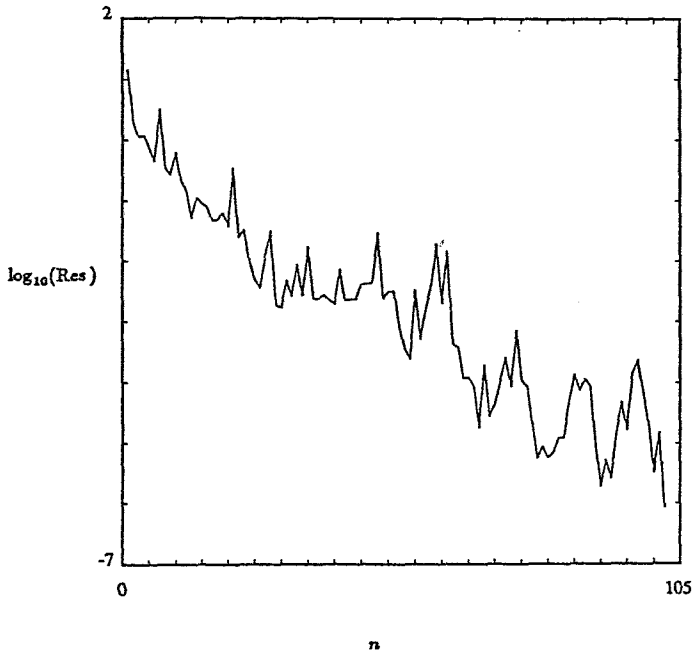

Figure 4.3

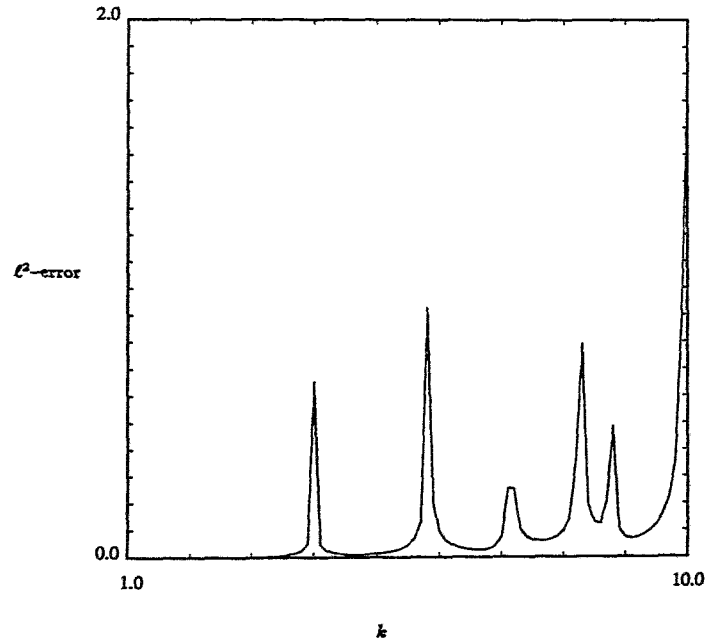

Figure 4.4(a)

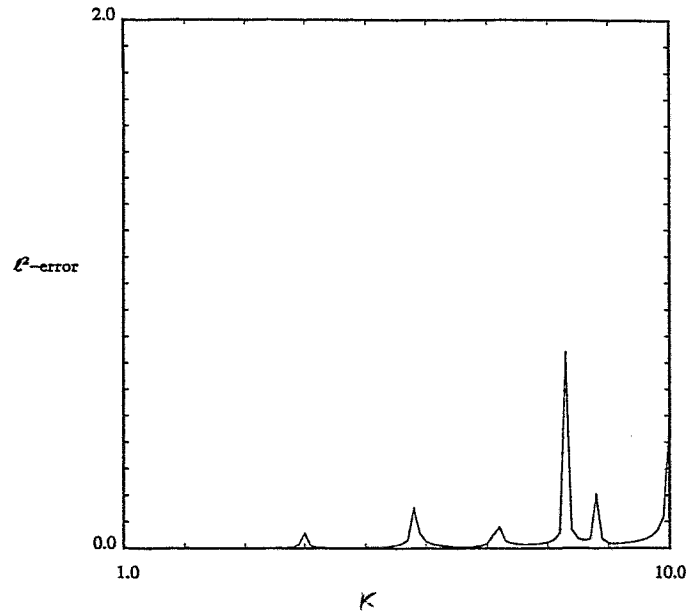

Figure 4.4(b)

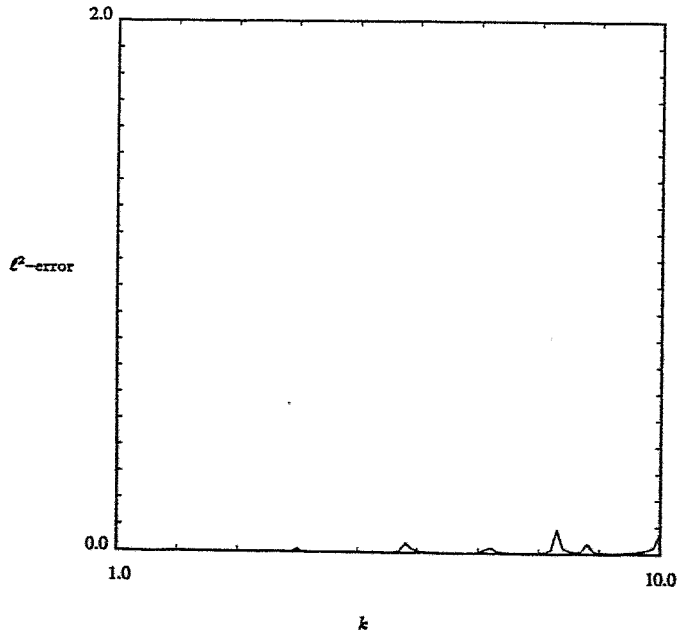

Figure 4.4(c)

h	$\|u - u_h\|_{L^2(\omega)}$	Iteration Number
1/16	7.1×10^{-2}	92
1/32	1.9×10^{-2}	204
1/64	4.8×10^{-3}	101

Table 4.1 (k=9, $\theta=\pi/4$)

It appears from Table 4.1 that our approximation is $O(h^2)$ and that the number of iterations necessary to achieve convergence seems to be independent of h away from the resonances. Finally, still for k=9 we have visualized on Figures 4.5(a), (b) the variations of u and u_h for k=9, h=1/64, $\theta=\frac{\pi}{4}$ along the horizontal and vertical diameters of A, respectively. The exact and computed results coincide with a very high accuracy.

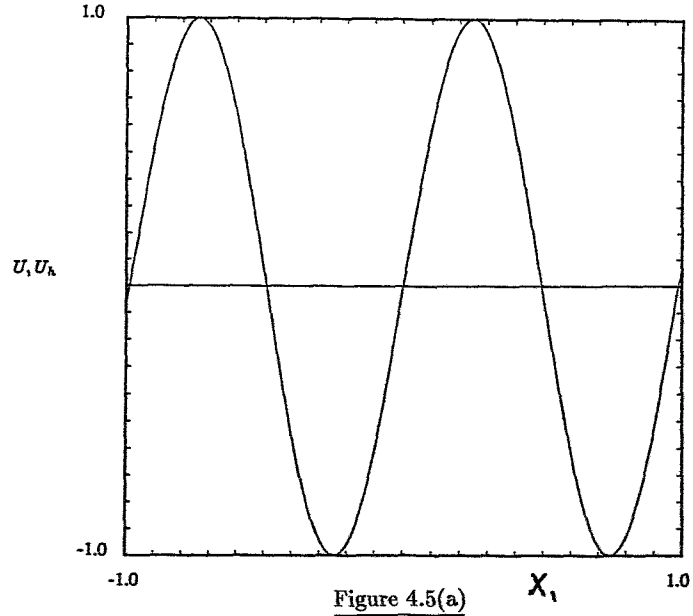

Figure 4.5(a)

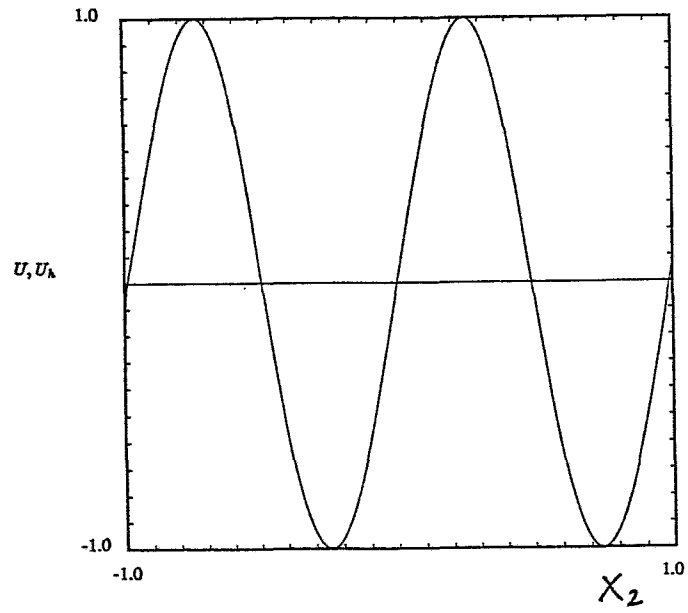

Figure 4.5(b)

4.5.3 A second test problem: The single ellipse case.

For this test problem, domain A is the interior of the ellipse $x_1^2+4x_2^2=1/16$; the great axis is therefore 1/2 long, while the small one is 1/4 long; domain Ω is again the square $(-1,1)\times(-1,1)$ as shown on Figure 4.6, together with a finite element grid corresponding to $h=1/16$. The exact solution is still defined by (4.35). For $k=9$, $\theta=\pi/4$ and $h=1/64$ the conjugate residual shown on Figure 4.7 looks like very much the one on Figure 4.3; the same conclusions hold.

On Figure 4.8(a), (b), (c) we have shown the variation of $\|u_h-u\|_{L^2(\omega)}$ versus k for $\theta=\pi/4$ and $h=1/16$, 1/32, 1/64, respectively. The stopping criterion is defined (with obvious notation) by

$$\|g_h^{n+1}\|_{V_h\times\Lambda_h} \Big/ \|g_h^o\|_{V_h\times\Lambda_h} \leq 10^{-7}. \tag{4.37}$$

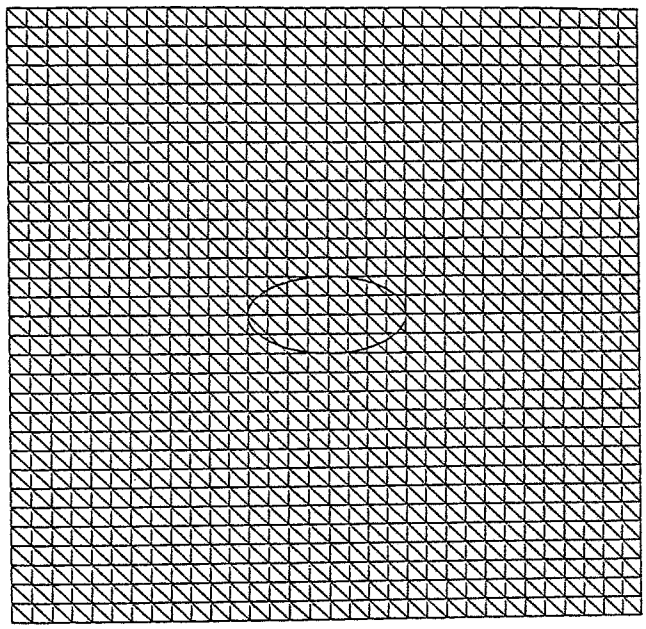

Figure 4.6

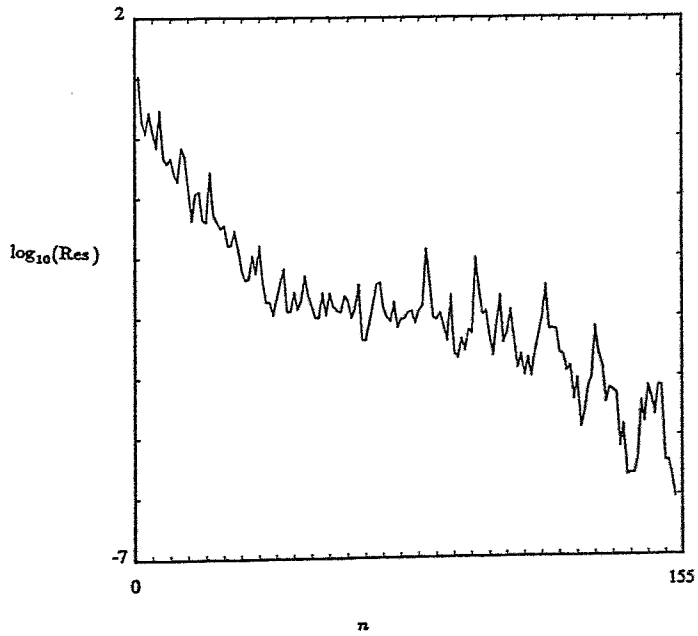

Figure 4.7

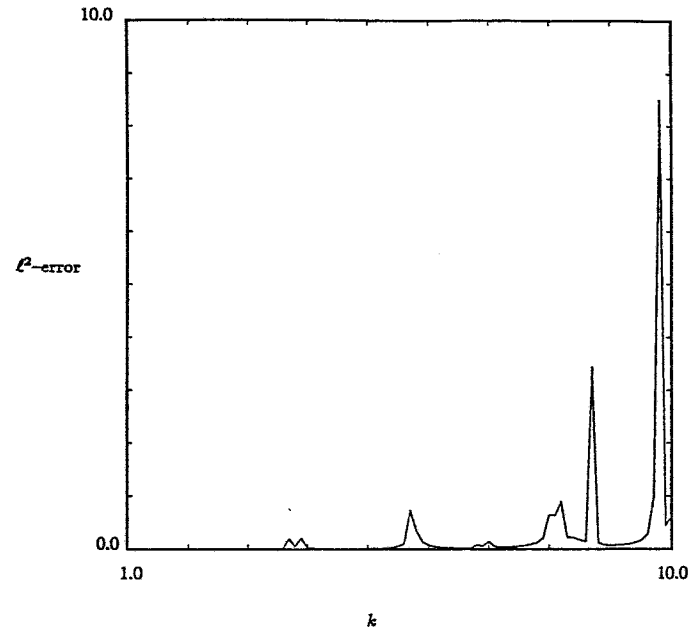

Figure 4.8(a)

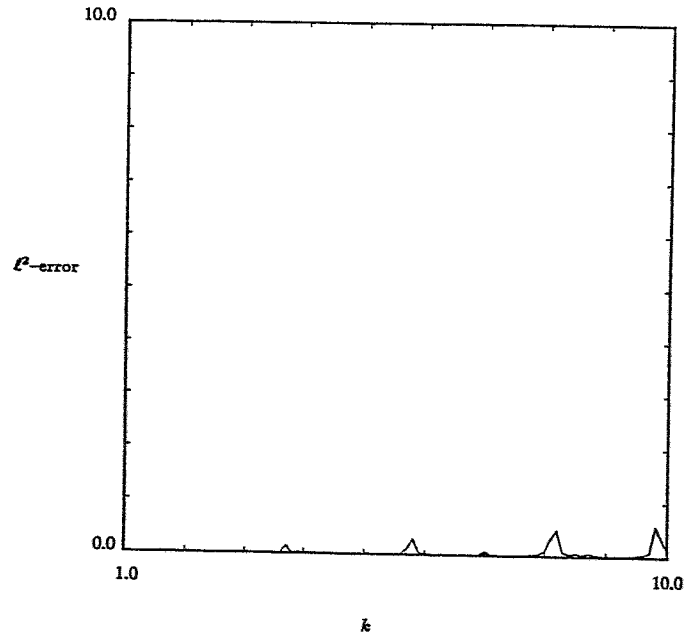

Figure 4.8(b)

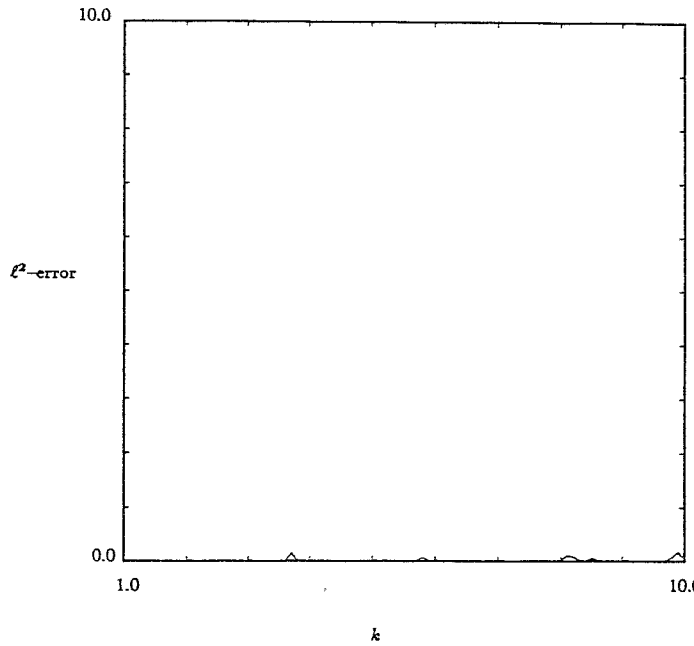

Figure 4.8(c)

We observe phenomena similar to those observed in Section 4.5.2 for the disk. Table 4.2, below exhibits the same qualitative behavior than Table 4.1. The number of iterations necessary for convergence is nevertheless higher; on the other hand the L^2-errors are smaller and still $0(h^2)$.

h	$\|u - u_h\|_{L^2(\omega)}$	Iteration Number
1/16	7.1×10^{-2}	142
1/32	1.7×10^{-2}	221
1/64	4.4×10^{-3}	152

Table 4.2

Actually, of one replaces 10^{-7} by 10^{-6} in (4.36) the iteration number may be substantially reduced. If one plots the variations of u_h and u along the horizontal and vertical axes of the ellipse for k=9, $\theta=\frac{\pi}{4}$ and h=1/64 once again we can not distinguish between approximate and exact solutions.

4.5.4 A third test problem: The double ellipse case.

For this test problem, domain A is the union of the interiors of the two ellipses whose equations are given (see Figure 4.9) by

$$x_1^2 + 4(x_2 - 3/16)^2 = 1/16 \text{ and } x_1^2 + 4(x_2 + 3/16)^2 = 1/16.$$

The distances between the two ellipses is 1/8. Domain A has been imbedded in $(-1,1)\times(-1,1)$ as shown on Figure 4.9, which also shows the finite element grid used for calculations (here h=1/32). For k=9, $\theta=\pi/4$ and h=1/64 the conjugate residual shown on Figure 4.10 looks like very much those on Figures 4.3 and 4.7. Table 4.3 shows the variations of $\|u_h-u\|_{L^2(\omega)}$ and of the number of iterations, versus h.

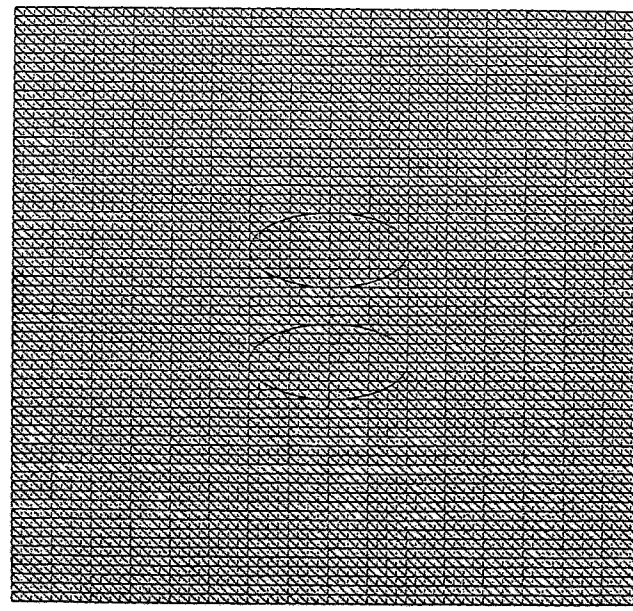

Figure 4.9

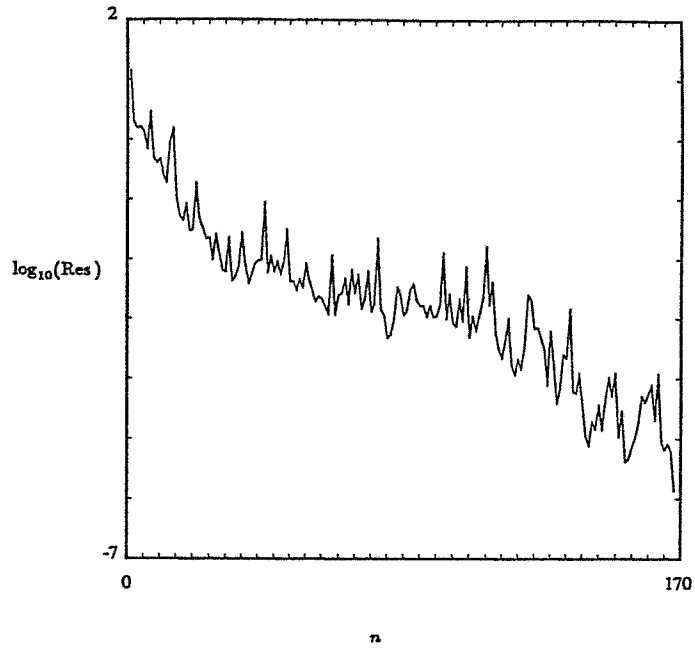

Figure 4.10

h	$\|u - u_h\|_{L^2(\omega)}$	Iteration Number
1/16	6.7×10^{-2}	239
1/32	1.7×10^{-2}	375
1/64	4.2×10^{-3}	167

Table 4.3

The above table shows that once again $\|u_h - u\|_{L^2(\omega)} = 0(h^2)$ and that the number of iteration seems to decrease with h. Figures 4.11 to 4.13 shows (for k=9, $\theta=\pi/4$, h=1/64) the variations of u_h and u on different lines of the plane $x_1 0 x_2$, namely the lines $x_1=0$, $x_2=0$ and $x_2=3/16$, respectively.

The coincidence between exact and approximate solution is (once again) excellent.

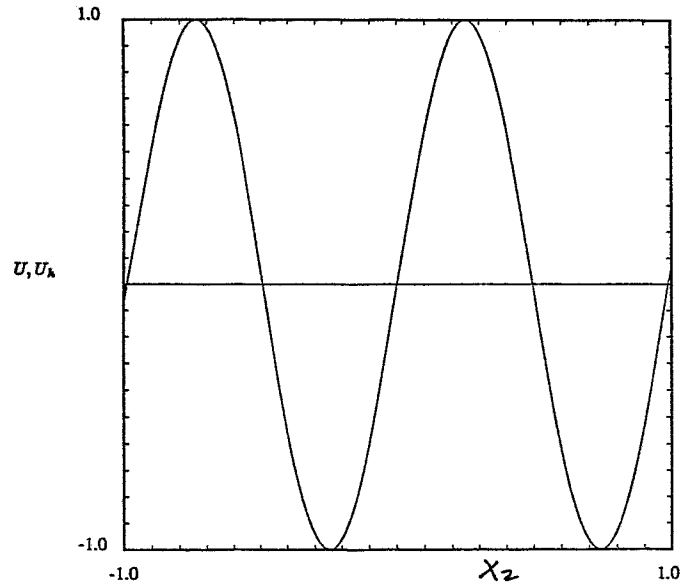

Figure 4.11

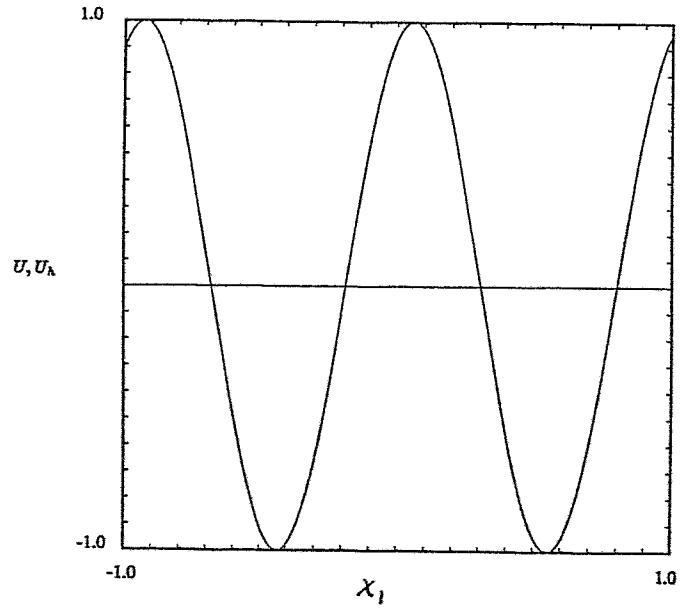

Figure 4.12

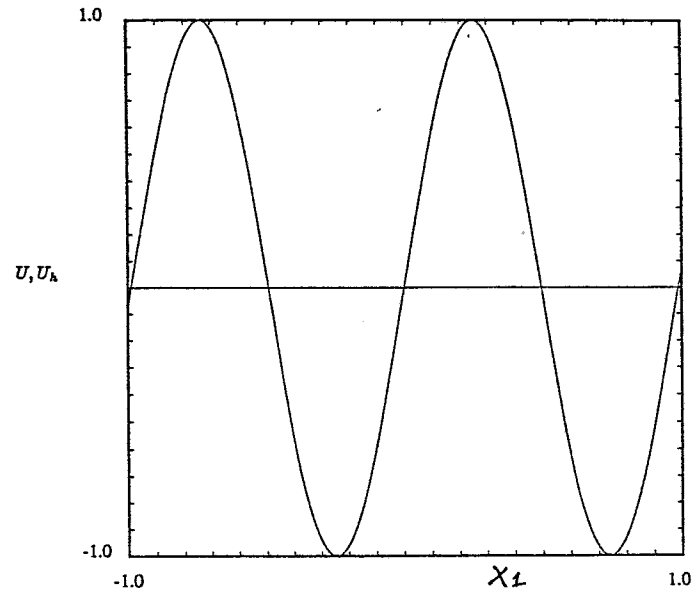

Figure 4.13

5. Conclusion.

The Lagrange multiplier/fictitious domain methodology discussed in this article improves from our point of view the closely related methodology discussed in [5] and [25]. The methods discussed here are closely related to the capacitance matrix methods discussed in e.g. [36], [37] (see also the references therein), with nevertheless more flexibility here concerning the use of the Lagrange multipliers. The concept is fully validated for elliptic Dirichlet problems and looks promising for Navier-Stokes and Helmoltz equations; progress however is still needed concerning better preconditioners. Application to Neumann type problems is discussed in the companion paper [38].

Acknowledgment

We would like to acknowledge the helpful comments and suggestions of the following individuals: C. Atamian, L. C. Cowsar, C. De la Foye, G. H. Golub, P. Joly, Y. Kuznetsov, A. Latto, W. Lawton, P. Le Tallec, J. L. Lions, P. L. Lions, G. Meurant, J. Pasciak, M. Ravachol, H. Resnikoff, H. Steve, J. Weiss, R. O. Wells, M. F. Wheeler, O. B. Widlund.

The support of the following corporations or institutions is also acknowledged: AWARE, Dassault Aviation, INRIA, University of Houston, Université Pierre et Marie Curie. We also benefited from the support of DARPA (Contracts AFOSR F49620-89-C-0125 and AFOSR-90-0334), DRET (Grant 89424) and NSF (Grants INT 8612680 and DMS 8822522). Finally, we would like to thank J. A. Wilson for the processing of this article.

References

[1] D. P. YOUNG, R. G. MELVIN, M. B. BIETERMAN, F. T. JOHNSON, S. S. SAMANTH, J. E. BUSSOLETTI, A locally refined finite rectangular grid finite element method. Application to Computational Physics, *J. Comp. Physics*, 92, (1991), pp. 1-66.

[2] B. L. BUZBEE, F. W. DORR, J. A. GEORGE, G. H. GOLUB, The direct solution of the discrete Poisson equation on irregular regions, *SIAM J. Num. Anal.*, 8, (1971), pp. 722-736.

[3] M. B. BIETERMAN et al, Solution adaptive local rectangular grid refinement for transonic aerodynamics flow problems, in *Proceedings of the 8th. GAMM Conference on Numerical Methods in Fluid Mechanics*, P. Wesseling ed., Notes on Numerical Fluid Mechanics, Vol. 29, Vieweg, Braunschweig, 1990.

[4] BORGERS, C., Domain imbedding methods for the Stokes equations, *Num. Math*, 57, (1990), 5, pp. 435-452.

[5] C. ATAMIAN, Q. V. DINH, R. GLOWINSKI, JIWEN HE, J. PERIAUX, Control approach to fictitious domain methods. Application to Fluid Dynamics and Electro Magnetics, in *Fourth International Symposium on Domain Decomposition Methods for Partial Differential Equations*, R. Glowinski, Y. Kuznetsov, G. Meurant, J. Periaux, O. B. Widlund eds., SIAM, Philadelphia, 1991, pp. 275-309.

[6] R. GLOWINSKI, P. LE TALLEC, *Augmented Lagrangian and Operator Splitting Methods in Nonlinear Mechanics*, SIAM, Philadelphia, 1989.

[7] M. DORR, On the discretization of interdomain coupling in elliptic boundary value problem, in *Domain Decomposition Methods*, T. F. Chan, R. Glowinski, J. Periaux, O. B. Widlund eds., SIAM, Philadelphia, 1989, pp. 17-37.

[8] R. W. HOCKNEY, A fast direct solution of Poisson's equation using Fourier Analysis, *J. Ass. Comp. Mach.*, 12, (1965), pp. 95-113.

[9] O. BUNEMAN, A compact non-iterative Poisson solver, Report 294, Stanford University Institute for Plasma Research, Stanford, Cal., 1969.

[10] R. A. SWEET, A generalized cyclic reduction algorithm, *SIAM J. Num. Anal.*, 11, (1974), pp. 506-520.

[11] R. A. SWEET, A cyclic reduction algorithm for solving block tridiagonal systems of arbitrary dimension, *SIAM J. Num. Anal.*, 14, (1977), pp. 706-720.

[12] P. N. SWARTZTRAUBER, R. A. SWEET, The direct solution of the discrete Poisson equation on a disk, *SIAM. J. Num. Anal.*, 10, (1973), pp. 900-907.

[13] D. HELLER, Some aspects of the cyclic reduction algorithm for block tridiagonal linear systems, *SIAM J. Num. Anal.*, 13, (1976), pp. 484-496.

[14] G. H. GOLUB, C. F. VAN LOAN, *Matrix Computations*, Johns Hopkin University Press, Baltimore, 1983.

[15] D. PEACEMAN, H. RACHFORD, The numerical solution of parabolic and elliptic differential equations, *J. SIAM*, 3, (1955), pp. 28-41.

[16] G. I. MARCHUK, *Methods of Numerical Mathematics*, Springer, New York, 1975.

[17] G. I. MARCHUK, *Splitting and Alternating Direction Methods*, in *Handbook of Numerical Analysis, Vol.* 1, P. G. Ciarlet, J. L. Lions (eds.), North Holland, Amsterdam, 1990, pp. 197-462.

[18] R. GLOWINSKI, Finite element methods for the numerical simulation of incompressible viscous flow. Introduction to the control of the Navier-Stokes equations, *Proceedings of the AMS Conference on Vortex Dynamics and Vortex Methods, Seattle, July* 1990, C. Anderson, C. Greengard (eds.), AMS, Providence (to appear).

[19] J. CAHOUET, J. P. CHABARD, Some fast 3D solvers for the generalized Stokes problem, *Int. J. Num. Meth. in Fluids*, 8, (1988), pp. 269-295.

[20] O. PIRONNEAU, *Finite Element Methods for Fluids*, J. Wiley, Chichester, 1989.

[21] R. DAUTRAY, J. L. LIONS (eds.), *Analyse Mathematique et Calcul Numerique*, I, *Modèles Physiques*, Masson, Paris, 1987.

[22] B. ENGQUIST, A. MAJDA, Absorbing boundary conditions for the numerical computation of waves, *Math. Comp.*, 31, (1977), pp. 629-651.

[23] B. ENGQUIST, A. MAJDA, Radiation boundary conditions for accoustic and elastic wave calculations, *Comm. Pure Appl. Math.*, 32, (1979), pp. 313-357.

[24] A. BAYLISS, E. TURKEL, Radiation boundary conditions for wave like equations, *Comm. Pure Appl. Math.*, 33, (1980), pp. 707-725.

[25] C. ATAMIAN, *Résolution de Problèmes de Diffraction d'Ondes Acoustiques et Electromagnétiques en Régime Fréquentiel par une Méthode de Domaines Fictifs*, Thesis, Université P. et M. Curie, May 1991.

[26] R. GLOWINSKI, J. L. LIONS, R. TREMOLIERES, *Numerical Analysis of Variational Inequalities*, North-Holland, Amsterdam, 1981.

[27] P. L. LIONS, Personal Communication, Los Angeles, 1988.

[28] I. M. NAVON et al, Numerical experience with limited-memory quasi-Newton methods for large-scale unconstrained minimization, Florida State University Supercomputer Computations Research Institute report FSU-SCRI-91-K, Tallahassee, Florida, 1991.

[29] M. O. BRISTEAU, R. GLOWINSKI, J. PERIAUX, P. PERRIER, O. PIRONNEAU, On the numerical solution of nonlinear problems in Fluid Dynamics by least squares and finite element methods (I). Least squares formulation and conjugate gradient solution of the continuous problems, *Comp. Meth. Appl. Mech. Eng.*, 17/18, (1979), pp. 619-657.

[30] M. O BRISTEAU, R. GLOWINSKI, J. PERIAUX, O. PIRONNEAU, P. PERRIER, G. POIRIER, On the numerical solution of nonlinear problems in Fluid Dynamics by least squares and finite element methods (II). Application to transonic flow simulations, *Comp. Meth. Appl. Mech. Eng.*, **51**, (1985), pp. 363-394.

[31] R. GLOWINSKI, *Numerical Methdos for Nonlinear Variational Problems*, Springer-Verlag, New York, 1984.

[32] R. GLOWINSKI, H. B. KELLER, L. REINHART, Continuation-Conjugate Gradient Methods for the Least-Squares Solution of Nonlinear Boundary Value Problems, *SIAM J. Scient. Stat. Comp.*, **6**, (1985), pp. 793-832.

[33] M. O. BRISTEAU, R. GLOWINSKI, J. PERIAUX, Numerical Methods for the Navier-Stokes equations, *Comp. Phys. Reports*, **6**, (1987), pp. 73-187.

[34] E. J. DEAN, R. GLOWINSKI, C. H. LI, Supercomputer solution of partial differential equations in Computational Fluid Dynamics and in Control, *Comp. Phys. Comm.*, **53**, (1989), pp. 401-439.

[35] F. X. ROUX, Acceleration of the Outer Conjugate Gradient by Reorthogonalization for a Domain Decomposition Methods with Lagrange Multiplier, in *Domain Decomposition Methods for Partial Differential Equations*, T. F. Chan, R. Glowinski, J. Periaux, O. B. Widlund eds., SIAM, Philadelphia, 1990, pp. 314-321.

[36] W. PROSKUROWSKY, O. B. WIDLUND, On the numerical solution of Helmholtz equation by the capacitance matrix method, *Math. Comp.*, **30**, (1979), pp. 433-468.

[37] D. P. O'LEARY, O. B. WIDLUND, Capacitance matrix methods for the Helmholtz equation on general three-dimensional regions, *Math. Comp.*, **30**, (1979), pp. 849-879.

[38] E. J. DEAN, Q. V. DINH, R. GLOWINSKI, JIWEN HE, T. W. PAN, J. PERIAUX, Least square domain imbedding methods for Neumann problems: Application to Fluid Dynamics (these proceedings).